Validation of Notch-Stress Intensity Factor, Strain Energy Density and Effective Notch Stress approaches in fatigue life assessment of austenitic steel welded joints

S. Marchetta, P. Corigliano, G. Palomba, G. Risitano, D. Santonocito
University of Messina, Department of Engineering, Messina, Italy
santi.marchetta@studenti.unime.it, https://orcid.org/0009-0002-5221-3553
pasqualino.corigliano@unime.it, https://orcid.org/0000-0003-0319-048X
giulia.palomba@unime.it, https://orcid.org/0000-0003-1996-0880
giacomo.risitano@unime.it, https://orcid.org/0000-0002-0506-8720
dariofrancesco.santonocito@unime.it, https://orcid.org/0000-0002-9709-9638

ABSTRACT. The purpose of this work is to validate the N-SIF (Notch-Stress Intensity Factor), SED (Strain Energy Density) and ENS (Effective Notch Stress) approaches for the fatigue design of austenitic stainless steel welded joints. Literature fatigue data for cruciform welded joints, originally expressed in terms of nominal stress, were first re-analysed through a finite element model in terms of N-SIF. The resulting fatigue limit was then used to determine the SED critical radius required for the application of the SED approach. The same dataset was subsequently reprocessed in terms of SED. Finally, a second finite element model was implemented to calculate the ENS values. The N-SIF and SED approaches led to a more unified representation of the fatigue behaviour compared to nominal stress, showing a noticeable reduction in data scatter. In contrast, the ENS method exhibited a significant dispersion for the investigated joints, possibly due to material-specific effects and to the geometric regularisation introduced by the fictitious notch radius. Although the available dataset is limited to root failures in cruciform joints, the results suggest promising applicability of fracture-mechanics-based local approaches to austenitic stainless steel welded joints, while indicating that further validation of the ENS method is required.

KEYWORDS. Austenitic steel welded joints, Notch-Stress Intensity Factor, Strain Energy Density, Effective Notch Stress, Finite element analysis.

OPEN ACCESS

Citation: Marchetta, S., Corigliano, P., Palomba, G., Risitano, G., Santonocito, D., Validation of Notch-Stress Intensity Factor, Strain Energy Density and Effective Notch Stress approaches in fatigue life assessment of austenitic steel welded joints, Fracture and Structural Integrity, 77 (2026) 298-315.

Received: 28.02.2026
Accepted: 21.05.2026
Published: 23.05.2026
Issue: 07.2026

INTRODUCTION

In welded joints, fatigue stands out as the principal damaging mechanism as the presence of several geometrical discontinuities, induced by the welding process, involves localized stress concentrations which can lead to crack initiation from different locations (toes and roots). In the course of time, several experimental and numerical

methodologies were developed to address the fatigue life problem in welded components [1,2]. Most of the international design codes [3–5] adopt the nominal stress criterium, which correlates the fatigue life with stress values calculated at the critical cross section. However, when nominal stress-based fatigue data related to different joint geometries are elaborated, a significant scatter is usually observed [6]. The nominal stress, in fact, does not account for the local stress field at weld toes and roots, which is the main responsible of the fatigue damage mechanism. To overcome this limitation, several numerical approaches have been developed over the past thirty years, in which fatigue life is expressed as a function of local parameters evaluated in the most critical regions of the joint. A widespread local approach in the design codes is the Effective Notch Stress (ENS) method, which estimates the highest elastic stress at the weld toe or root by assuming a fictitious radius instead of the actual tip [7]. Alongside the ENS, literature reports other local methodologies based on linear elastic fracture mechanics and strain energy. The Notch-Stress Intensity Factor (N-SIF) approach, developed by Lazzarin and Tovo [6], models weld toes and roots as sharp V-notches and applies notch stress intensity factors (based on fracture mechanics concepts originally developed for cracks [8] and subsequently extended to V-notches [9]) to express the fatigue life of welded joints in terms of the local asymptotic stress field. Alternatively, the Strain Energy Density (SED) approach, introduced by Lazzarin and Zambardi [10], relates fatigue behaviour to the elastic strain energy density averaged within a finite material volume around the notch tip, thus adopting an energy-based parameter instead of a stress-based one.

The described methodologies allow a coherent comparison between fatigue data relative to components characterised by different geometries, loading ratios and boundary conditions and have been validated for various materials such as structural steel [11], aluminium [12], titanium [13] and PMMA [10].

Despite the extensive validation of local approaches for structural steels, aluminium alloys and other materials, their applicability to austenitic stainless steel welded joints remains limited and not fully understood. Austenitic steels exhibit different mechanical behaviour compared to conventional structural steels, including higher ductility and potentially different notch sensitivity, which may influence fatigue performance and the reliability of local fatigue parameters. Consequently, the transferability of methodologies such as ENS, N-SIF and SED to this class of materials cannot be assumed a priori and requires dedicated assessment.

In this context, the present work aims to assess the applicability of ENS, N-SIF and SED approaches to the fatigue assessment of welded joints made of austenitic stainless steel. Literature fatigue data on austenitic steel welded joints were re-analysed through finite element modelling (FEM) in order to evaluate the corresponding local parameters and to compare the resulting data scatter with that obtained using nominal stress.

MATERIALS AND METHODS

This section provides a theoretical background of the numerical methodologies employed in the following study.

Notch-Stress Intensity Factor (N-SIF)

The Notch-Stress Intensity Factor (N-SIF) approach proposed by Lazzarin and Tovo [6] represents one of the earliest attempts to unify the fatigue assessment process of welded joints characterized by different geometries and size scales. This methodology consists in determining the stress distribution field in the neighbourhood of weld toes and roots.

Before introducing the adopted numerical procedure, some basic concepts of linear elastic fracture mechanics are briefly recalled. Under the hypothesis of plane strain conditions, the stress field in the vicinity of a crack tip can be expressed as the superposition of two independent stress intensity factors:

- Mode I (Opening): Tensile stress normal to the crack plane.
- Mode II (Sliding): Shear stress parallel to the crack plane.

Fig. 1 summarizes the loading conditions described above.

Gross and Mendelson [9] extended the application of the intensity factor to the evaluation of stress fields in the vicinity of sharp V-notches, leading to the following expressions for the Notch-Stress Intensity Factors:

$$K_1=\sqrt{2\pi}\lim_{r\to 0^+} r^{1-\lambda_1}(\sigma_{\vartheta\vartheta})_{\vartheta=0} \quad (1)$$

$$K_2=\sqrt{2\pi}\lim_{r\to 0^+} r^{1-\lambda_2}(\tau_{r\vartheta})_{\vartheta=0} \quad (2)$$

where $\sigma_{\vartheta\vartheta}$ and $\tau_{r\vartheta}$ are the stress components in a cylindrical coordinate system centred at the notch tip and with the abscissa axis oriented along the notch bisector (see Fig. 2), *r* is the distance from the notch tip and λ_1 and λ_2 are the Williams' eigenvalues [8], which correlate the notch opening angle 2α with the stress field at the tip. For 2α>102.5°, the Mode II eigenvalue λ_2 exceeds unity, leading to a non-singular stress field in shear, independently of the loading mode.
Due to the singular nature of the stress field, N-SIF values calculated exactly at the notch tip are not physically meaningful, as they are affected by the stress singularity and tend to diverge. Conversely, stress data extracted at distances too far from the notch tip are no longer representative of the asymptotic notch stress field.

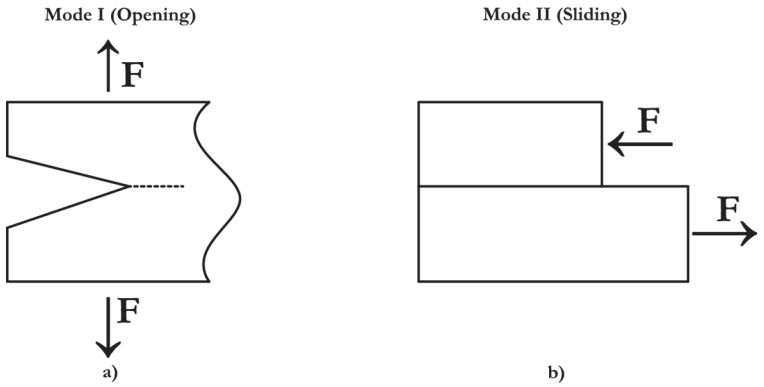

Figure 1: Crack loading modes in plane strain conditions; a) Opening, b) Sliding.

Accordingly, the evaluation of K_1 and K_2 was performed within a radial distance range from the notch tip between 10^{-4} mm and 10^{-2} mm, where a plateau of nearly constant values was observed.

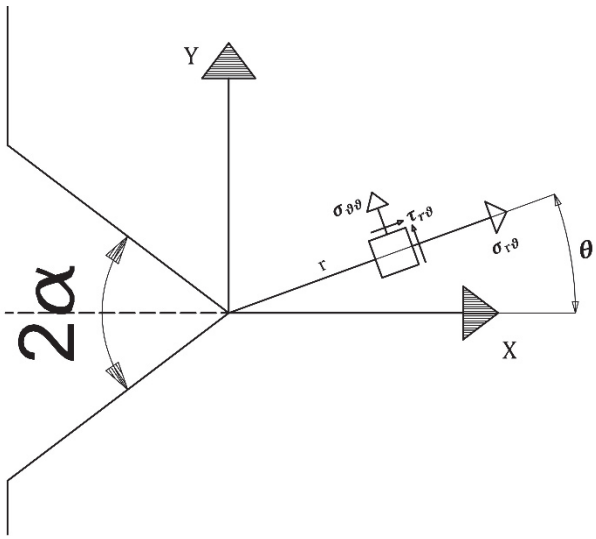

Figure 2: Coordinate system for N-SIF calculations in sharp V-notches (adapted from [6]).

By treating weld toes and roots as sharp V-notches it is possible to determine the local stress intensity fields by using Eqn. 1 and Eqn. 2. The calculation of $\sigma_{\vartheta\vartheta}$ and $\tau_{r\vartheta}$ is carried out by means of a finite element model with a highly refined mesh in the neighbourhood of the weld toe/root (element dimension close to 10^{-5} mm).
When fatigue strength data of welded joints with different characteristic dimensions are re-analysed in terms of N-SIF it is possible to observe a significant reduction in data scatter [6] compared to that of the experimental data, expressed in terms of nominal stress. This reflects the dominant role of the local stress field in governing fatigue crack initiation at weld notches. However, the N-SIF measuring unit is MPa* $mm^{(1-\lambda_1)}$, where λ_1 is the Mode I Williams' eigenvalue, which depends on the notch opening angle 2α. Consequently, a direct comparison between values calculated at weld toes (where typically 2α=135°,

leading to MPa·mm$^{0.236}$) and weld roots (2α=0°, MPa·mm$^{0.5}$) is meaningless, since the coherence in the physical dimensions would be lost. The criterion discussed in the next paragraph allows to overcome the limitations of this method.

Strain Energy Density (SED) approach

The Strain Energy Density (SED) approach, presented for the first time by Lazzarin and Zambardi [10], enables a meaningful comparison between geometries with different values of 2α and can be used to predict both the static and fatigue behaviour of notched components. As its name suggests, the criterion adopts the strain energy density W averaged within a finite material volume V_0 (A-SED) surrounding the critical region under investigation, as the parameter for structural strength assessment. The basic assumption of this method is that, under linear elastic conditions, brittle failure mechanisms and isotropic material, failure will occur when the average local SED $\bar{W}$ reaches a critical value $\bar{W}_N$ which depends exclusively on the material.

Dealing with fatigue phenomena, the critical cyclic averaged SED $\Delta\bar{W}_N$ of a smooth specimen can be estimated from the following equation [10]:

$$\Delta\bar{W}_N = \frac{\Delta\sigma_A^2}{2E} \tag{3}$$

where $\Delta\sigma_A$ is the fatigue limit of the material and E is the Young's modulus.

The control volume is defined by a shape, dependent on the geometry of the investigated detail, and a characteristic length R_C, which is a material property. In the case of a sharp V-notch or a crack, the volume is a circular sector of radius R_C (see Fig. 3). Moreover, the approach can be extended to blunt V-notches and U-notches under both pure Mode I and mixed modes loading conditions. In these cases, the control volume assumes a crescent shape. Further details on the definition and positioning of the control volume for these configurations can be found in [14].

In a similar way to what was seen with the N-SIF approach, by modelling weld toes and roots as notches, this methodology can be applied to evaluate the strength of welded structures.

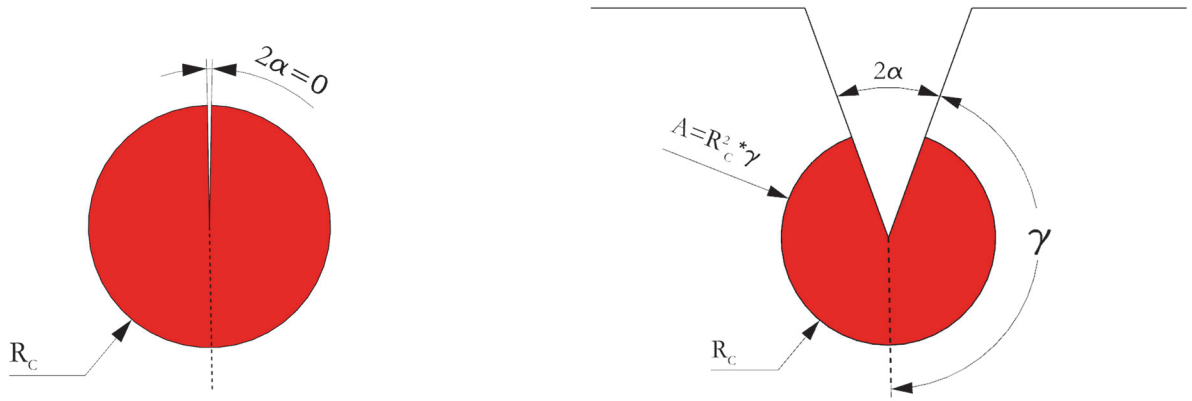

Figure 3: SED control volumes; a) crack, b) sharp V-notch (adapted from [14]).

The analytical formulation of $\Delta\bar{W}$ for a notched specimen, in plane strain conditions [10], is correlated to Mode I and Mode II N-SIF defined in Eqn. 1 and Eqn. 2:

$$\Delta\bar{W} = \frac{1}{E}\left(e_1 \cdot \frac{\Delta K_{1A}^2}{R_C^{2(1-\lambda_1)}} + e_2 \cdot \frac{\Delta K_{2A}^2}{R_C^{2(1-\lambda_2)}} \right) \tag{4}$$

where e_1 and e_2 [15] are two functions dependent on the notch opening angle 2α, ΔK_{1A} and ΔK_{2A} are respectively the Mode I and Mode II fatigue limits expressed in terms of N-SIF, λ_1 and λ_2 are the Williams' eigenvalues.

In the case of pure Mode I external loads or notch opening angle 2α>102.5, Eqn. 4 can be simplified as follows:

$$\Delta\bar{W}=\frac{1}{E}\left(e_1\cdot\frac{\Delta K_{1A}^2}{R_C^{2(1-\lambda_1)}}\right) \tag{5}$$

The critical radius R_C can be estimated by equating the SED value associated to the plain specimen, seen in Eqn. 3, and the one of the notched specimens, reported in Eqn. 5, both evaluated at the fatigue limit or at a specified number of cycles. When dealing with welded joints, the fatigue limit to be taken into account for the calculation of $\Delta\bar{W}_N$ is that of butt ground welded joints, to avoid any possible stress concentration effect induced by the weld bead and to consider only the influence of the welding process on the fatigue properties of the material.
The final expression is:

$$R_C=\left(\sqrt{2e_1}\cdot\frac{\Delta K_{1A}}{\Delta\sigma_A}\right)^{\frac{1}{1-\lambda_1}} \tag{6}$$

An alternative method proposed by Crisafulli et al. [16] consists in evaluating R_C iteratively by applying the experimental fatigue limit load to a given geometry and varying the control radius until the following condition is met:

$$\Delta\bar{W}(R_C)=\Delta\bar{W}_N=\frac{\Delta\sigma_A^2}{2E} \tag{7}$$

Once R_C is evaluated, the SED approach can be applied in any potential crack initiation site of a welded joint. This method, if properly calibrated, offers several advantages over the N-SIF based one. The first is the possibility to directly compare data associated with failures initiating at the weld toe with those originating from the weld root, since the results are expressed in the same physical units, i.e. those of an energy density (MJ/m^3 or Nmm/mm^3), leading to a reduced scatter of fatigue data compared to nominal-stress-based representations [12].
The approach includes the effect of load ratio R by adopting the following equations [17]:

$$\Delta\bar{W}_R=c_w\cdot\Delta\bar{W}_0=\frac{1-R^2}{(1-R)^2}\Delta\bar{W}_0 \qquad \text{for } 0\le R\le 1 \tag{8}$$

$$\bar{W}_R=c_w\cdot\Delta\bar{W}_0=\frac{1+R^2}{(1-R)^2}\Delta\bar{W}_0 \qquad \text{for } -\infty\le R\le 1 \tag{9}$$

Moreover, the Strain Energy Density has an intrinsically finite value, as it represents an energy averaged over a small control volume defined in proximity to the structural detail, in contrast to the N-SIF, which relies on stress fields that are singular at the notch tip [10]. Moreover, while assuming a zero weld toe radius is often reasonable in practice, some welding procedures produce a finite mean toe radius, under which N-SIF-based predictions may underestimate fatigue life [18]. Finally, the mesh required for SED evaluation is significantly less refined than that needed for N-SIF calculations, as an accurate estimate of the parameter can be obtained with a relatively coarse mesh within the control volume [11].

Effective Notch Stress (ENS) approach

The Effective Notch Stress (ENS) approach, included in the IIW Recommendations [3], differs from the local approaches discussed above. Assuming linear elastic material behaviour, the methodology consists in evaluating, by means of finite element analysis, the maximum principal stress at weld roots. To account, in an effective manner, for weld bead variability and local non-linear effects at the notch root, the actual weld bead geometry is modified by the introduction of a fictitious and idealized weld profile. Fig. 4 illustrates the weld bead modelling suggestions proposed by the guidelines. In the case of ENS valuation at the weld root, the weld profile can be modelled as a keyhole notch (left) or a U-shaped notch (right). For this specific study, the U-shape idealization was chosen. A fictitious radius r= 1 mm has been found to lead to the most consistent results for structural steel and aluminium alloys welded joints. Furthermore, the IIW prescribes specific mesh

size requirements, consisting in 5 or more elements for every 45° arc in the case of linear element meshing, with an absolute minimum size of 0.15 mm, for finite element implementations of the ENS.
It is worth noting that this method is restricted to assessment of naturally formed as-welded weld toes and roots.

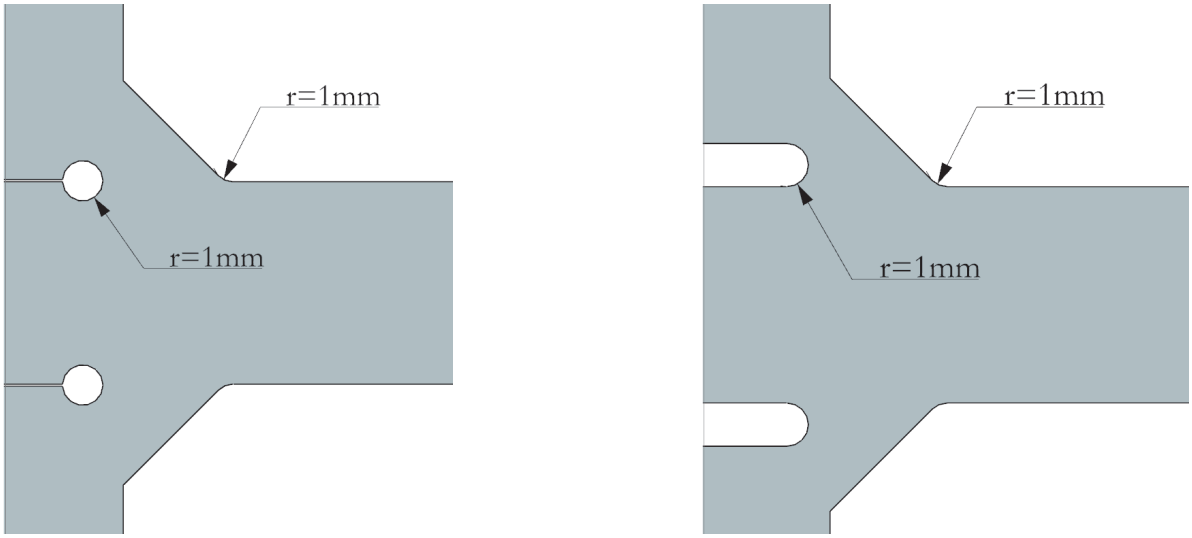

Figure 4: Recommended weld bead modelling for Effective Notch Stress evaluation (adapted from [3]).

Once evaluated, the guidelines prescribe to compare the obtained ENS values with the fatigue resistance classes (FAT curves) provided by the IIW. The approach can be regarded as safe for fatigue design purposes if the ENS values fall on, or above, the recommended FAT curve for the investigated joint. In the case of structural steel welded joints, the IIW suggests the FAT 225 as reference.
Compared to the approaches described previously, ENS generally requires less modelling effort, but its applicability is strongly influenced by the joint geometry. According to IIW Recommendations, the method is, in fact, limited to joints characterized by a plate thickness a,t ≥ 5 mm, since the method has not yet been verified for smaller thicknesses.

DATA GATHERING AND NUMERICAL SIMULATIONS

Literature survey

The finite element model calibration, starting from the N-SIF calculation to the definition of the critical radius R_C for the subsequent implementation of the SED criterion, was performed by using the fatigue data for austenitic steel welded joints available in the literature.
The data required for this calibration procedure are as follows:

- The fatigue limit of smooth welded specimens, $\Delta\sigma_A$
- S-N curves of notched welded specimens, associated with fully documented specimen geometries

Several studies in the literature report fatigue data for notched welded specimens; however, in most cases the corresponding geometric information is incomplete or insufficient for a reliable reconstruction of the tested details.
Tab. 1 reports a list containing the fatigue data of butt ground welded joints. GMAW stands for gas metal arc welding, GTAW stands for gas tungsten arc welding. NIMS data were collected from the work by Peng et al. [23]. The following data were analysed to find the mean S-N curve (P.S.=50%) and its corresponding fatigue limit at $2x10^6$ cycles $\Delta\sigma_{A,50\%}$ and the scatter band amplitude T_σ, considering a survival probability P.S. of 97.7%. A scatter plot of the data is available in Fig. 5, in which the slope values k highlighted in black correspond to the negative inverse slope of the mean curves obtained through free linear regression of the experimental data, whereas the magenta values indicate the negative inverse slope of the IIW FAT classes (k=3). In this case, both a free and forced linear regressions were performed. In the free regression, both the slope and intercept were determined from the experimental data, while in the forced regression the slope was fixed to k=3. This comparison allows the experimental trends to be directly compared with the fatigue design curves proposed by the standards. The fatigue limit was then estimated from the mean curve obtained through free regression. Further details regarding the statistical analysis procedure are provided in the dedicated section.

Welded joint type	Source	Austenitic steel type	Welding process	Load ratio, R
Butt ground	NIMS [19]	SUS304	-	0
	Nakamura et al. [20]	SUS304	-	0
	Branco et al. [21]	304L	GMAW	0.1
	Singh et al. [22]	304L	GMAW-GTAW	0

Table 1: Literature fatigue data test for austenitic steel butt ground welded joints.

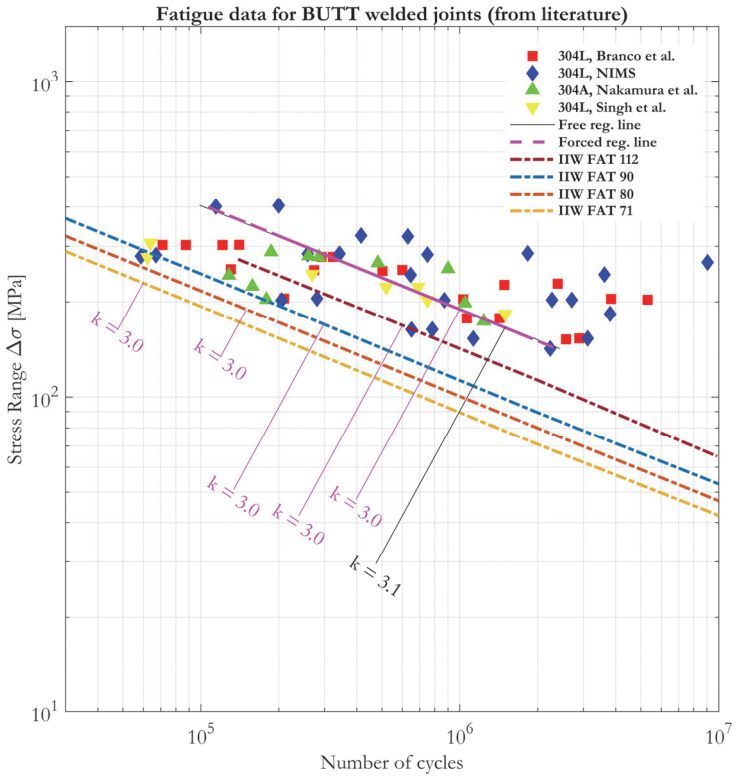

Figure 5: Scatter plot of butt-welded joints fatigue data.

Tab. 2 lists the references from which the joint geometries were extracted. All the analysed specimens are load-carrying cruciform welded joints with lack of penetration (LOP) defects under tensile load, with fatigue cracks initiating at the weld root. The table also contains all the geometric parameters. For a better understanding of the joint dimensions, refer to Fig. 6. The restriction to load-carrying cruciform joints with root failures and LOP defects was dictated by data availability, as no other literature datasets providing sufficiently detailed geometric information were found.

Welded joint type	Source	Austenitic steel type	Welding process	Load ratio, R	a [mm]	t [mm]	b [mm]	2α [°]	L1 [mm]	L2 [mm]	LOP [mm]	E [GPa]	ν
Cruciform-LC	Singh et al.[23]	304L	GMAW	0	6	6	4	120	50	100	4	202	0.3
	Peng et al.[24]	SUS304	GTAW	0.1	10	10	8	135	50	140	9.94	202	0.3
	Singh et al.[25]	304L	GTAW	0	6	6	4	150	50	100	2 3 4 6	202	0.3

Table 2: Literature fatigue data test for austenitic steel cruciform welded joints.

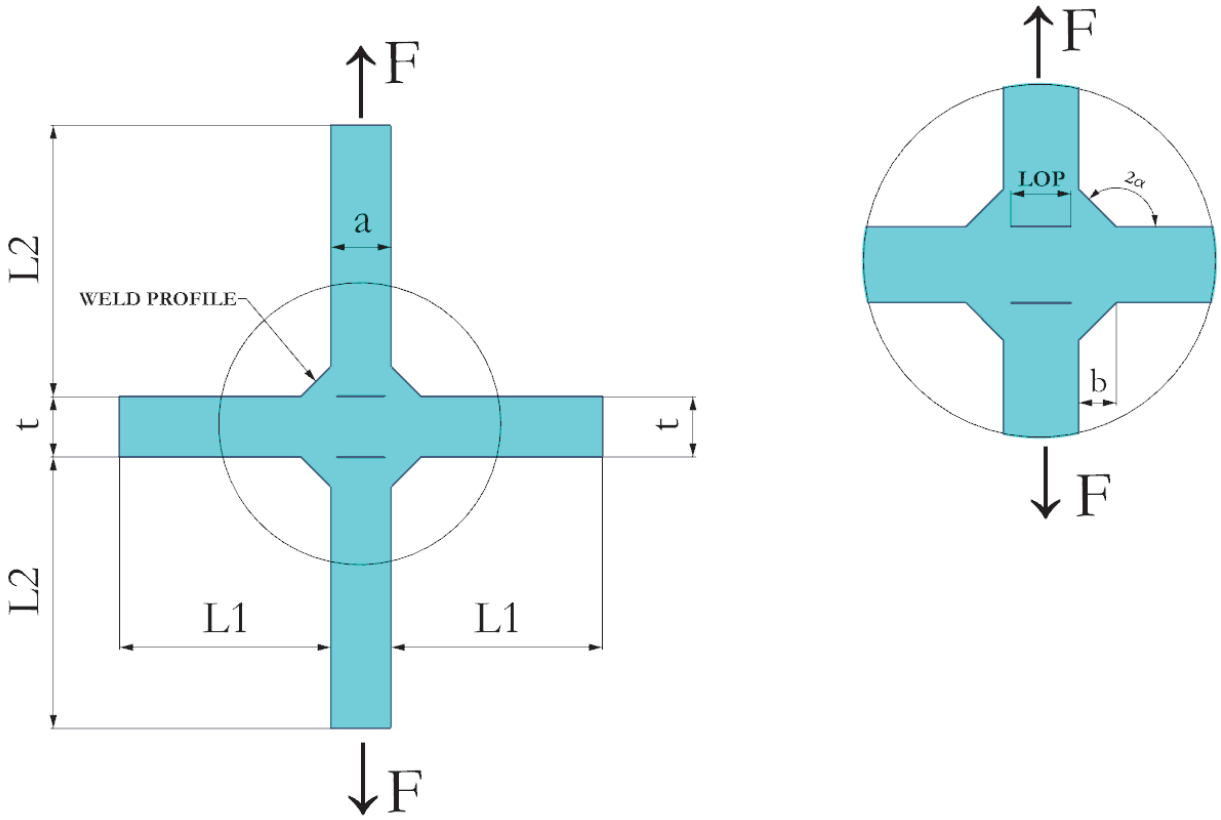

Figure 6: Cruciform-LC joint dimensions and experimental setup.

Finite Element Modelling (FEM)

2-D parametric finite element models were realized in Ansys® APDL to carry out all the simulations.

The first model allows the calculation of both the N-SIF and SED (Fig. 7). The system was modelled under plane strain condition adopting quadrilateral 4-node elements of the type PLANE182. Moreover, symmetry was applied (only a quarter of the joint geometry was modelled) to reduce time and computational costs. The weld root was modelled as a sharp V-notch (Fig. 3a) with an opening angle of 2° to avoid numerical instability. The notch is predominantly subjected to Mode I loading conditions, with a negligible influence of the Mode II component ΔK_2 on the resulting values. . As can be seen in Fig. 7, the geometry is divided into multiple areas. A mapped mesh for SED calculation was adopted in the area circled in red of radius R_C. Although SED can be accurately estimated with a limited number of elements within the control area, a finer mesh (800 elements) was employed to favour a progressive refinement toward the region of radius 10^{-4} mm highlighted in yellow, dedicated to the N-SIF evaluation, with further refinement in the vicinity of the weld root notch (element size of 10^{-5} mm). Finally, the rest of the joint was discretized with a free mesh of size t/10.

For every simulation, the finite element model extracts the elastic strain energy stored in the elements within the circular sector of radius R_C and the volume (m^3) of the circular sector itself. The cyclic average SED values $\Delta\bar{W}$ are then calculated by dividing the total strain energy for the volume of the circular sector (MJ/m^3).

The evaluation of $\Delta\bar{W}$ inherently accounts for the contribution of all stress components, since the SED is computed directly from the finite element solution and averaged over the control volume. In the case of the analysed joints, the Mode II contribution was found to be negligible due to the predominantly opening-mode loading conditions. However, the same methodology can be directly applied to more complex multiaxial loading scenarios, where both Mode I and Mode II contributions would be fully captured in the SED evaluation.

A different model for the ENS calculation was realized (Fig. 8). In this case, the weld root was modelled according to the IIW recommendations reported in Fig. 4. As prescribed by the guidelines, a mesh refinement was executed at the notch radius to assure at least 20 elements along it. Same element type, conditions, loads and constraints as the previous model were applied.

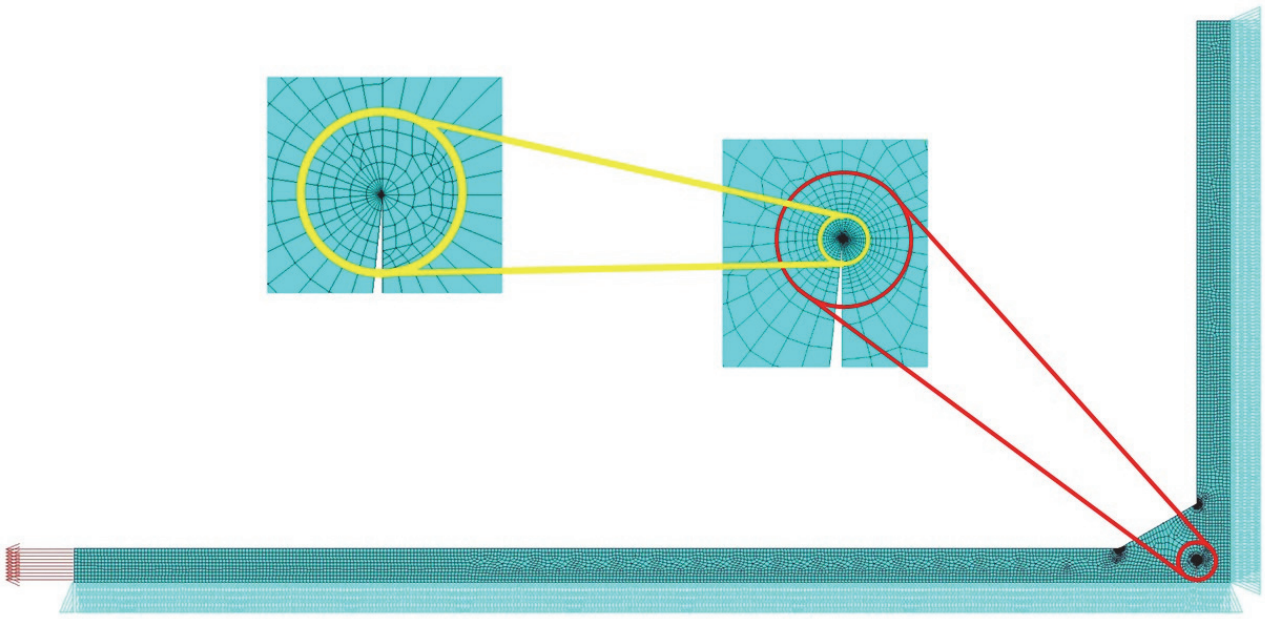

Figure 7: Finite element model for N-SIF and SED calculation.

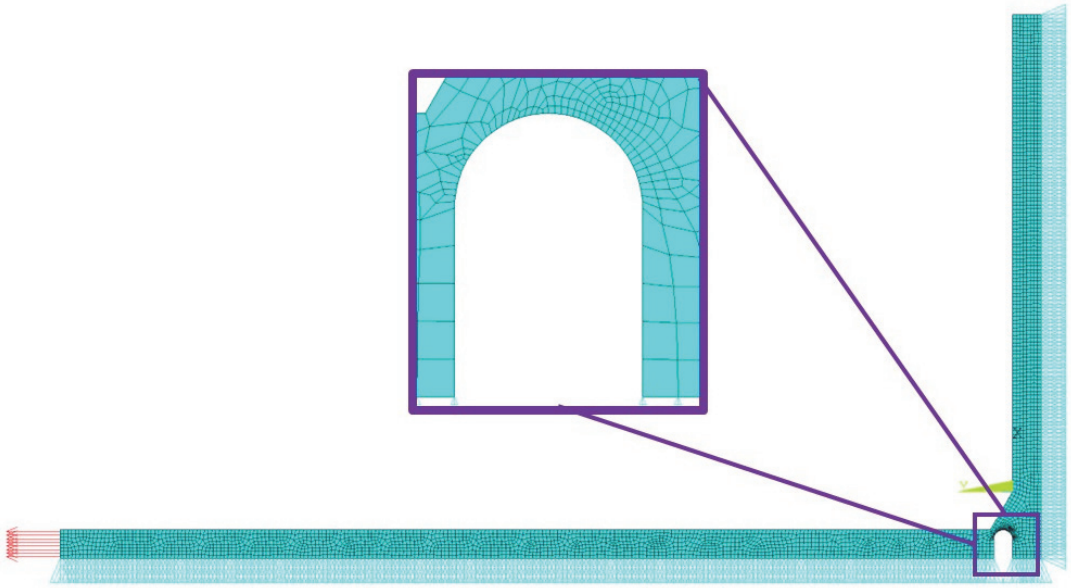

Figure 8: Finite element model for ENS calculation.

Statistical analysis

To determine the fatigue limit in terms of nominal stress and N-SIF, as well as the corresponding mean S–N curves and associated scatter bands for the different representations considered, the fatigue data were subjected to statistical analysis. As prescribed by the IIW Recommendations, a Gaussian log-normal distribution was assumed [3].

The S-N mean curve (P.S. 50%) is obtained by performing a linear regression on the fatigue data, in which log(N) is taken as the dependent variable, and is described by the following equation:

$$\log(N) = B \cdot \log(\sigma) + A \tag{10}$$

In which B is the inverse slope of the S-N curve and A is the intercept at σ=1 MPa (log(σ)=0):

$$B=\frac{\sum_{i=1}^{n}(\log(\sigma_i)-\log(\bar{\sigma}))(\log(N_i)-\log(\bar{N}))}{\sum_{i=1}^{n}(\log(\sigma_i)-\log(\bar{\sigma}))^2} \quad (11)$$

In fatigue literature, the parameter commonly reported is the negative inverse slope of the S–N curve, k, defined as:

$$k = - B \quad (12)$$

with $\bar{\sigma}$ being the mean stress and $\bar{N}$ the mean number of cycles:

$$\bar{\sigma}=\frac{1}{n}\sum_{i=1}^{n}\sigma_i \quad (13)$$

$$\bar{N}=\frac{1}{n}\sum_{i=1}^{n}N_i \quad (14)$$

The standard deviation s_x is defined as follows:

$$s_x=\sqrt{\frac{\sum_{i=1}^{n}(\log(\sigma_i)-\log(\bar{\sigma}))^2}{n-1}} \quad (15)$$

Once the mean S-N curve is obtained, the fatigue limit is evaluated at $2x10^6$ cycles. This reference value was selected since the analysed datasets exhibit a tendency towards a plateau around this number of cycles.
In fatigue data analysis, a commonly adopted approach is based on the two-standard-deviation criterion [3], which consists in constructing the upper and lower bounds of the scatter band by shifting the mean curve (P.S. 50%) by $\pm 2s_x$. However, as pointed out by Dowling [26], the direct use of the normal distribution in the estimation of probability limits on materials properties can lead to inaccuracy (unless dealing with very large sample sizes), since the sample mean $\bar{\sigma}$ and the standard deviation s_x represent estimates of the true population parameters (infinite number of observations).
To account for this additional source of statistical error, the bounds of the scatter bands were defined by using one-sided tolerance limits, shifting the mean curve as follows:

$$\sigma_{P.S.,C}=\bar{\sigma} \pm k_{P.S.,C} \cdot s_x \quad (15)$$

where $k_{P.S,C}$ is the one-sided tolerance limit factor, which depends on the sample size n, on the survival probability P.S. and on the confidence level C (such as 90%, 95% or 99%). A confidence level C=95% means that there is a 95% chance that the survival probability P.S. is satisfied. The one-sided tolerance limit factor can be calculated following the procedure provided by Natrella [27].
Finally, the scatter band amplitude T_σ is calculated as the ratio between the upper and lower scatter band stress values at a given number of cycles:

$$T_\sigma=\frac{\sigma_{sup}}{\sigma_{inf}} \quad (16)$$

Workflow

The flowchart displayed in Fig. 9 provides a comprehensive overview of the proposed workflow. After having acquired sufficiently complete fatigue data on both plain and notched welded specimens, a first set of simulations is carried out in order to obtain the ΔK_1 values for each configuration and to express the fatigue life in terms of N-SIF. The acquired results are then submitted to statistical analysis to find the data scatter band (PS 97.7%), the free mean fatigue design curve (P.S. 50%) and its corresponding fatigue limit at $2x10^6$ cycles, ΔK_{1A}. An identical procedure is executed on the fatigue data of butt ground welded joint to estimate the fatigue limit of the plain welded material in terms of nominal stress, $\Delta\sigma_{A,50\%}$. The

critical radius R_C can be now evaluated either by applying Eqn. 6 or the "iterative" method. Once R_C is calculated and applied to the finite element model, a second set of simulations is conducted to calculate the corresponding SED values. Simulations are also carried out with the model presented in Fig. 8 to calculate the ENS. Finally, a comparison between fatigue data expressed in terms of nominal stress, N-SIF, SED and ENS is made to verify the coherence of the results and the applicability of the methods for the investigated type of welded joints. In line with previous studies conducted on structural steel, Duraluminium and polymethyl methacrylate (PMMA) [6,10,15], a reduction in data scatter T_σ is expected when fatigue results are expressed in terms of NSIF and SED instead of nominal stress. Moreover, as anticipated, ENS fatigue data should align with the FAT class suggested by the IIW guidelines, namely FAT 225.

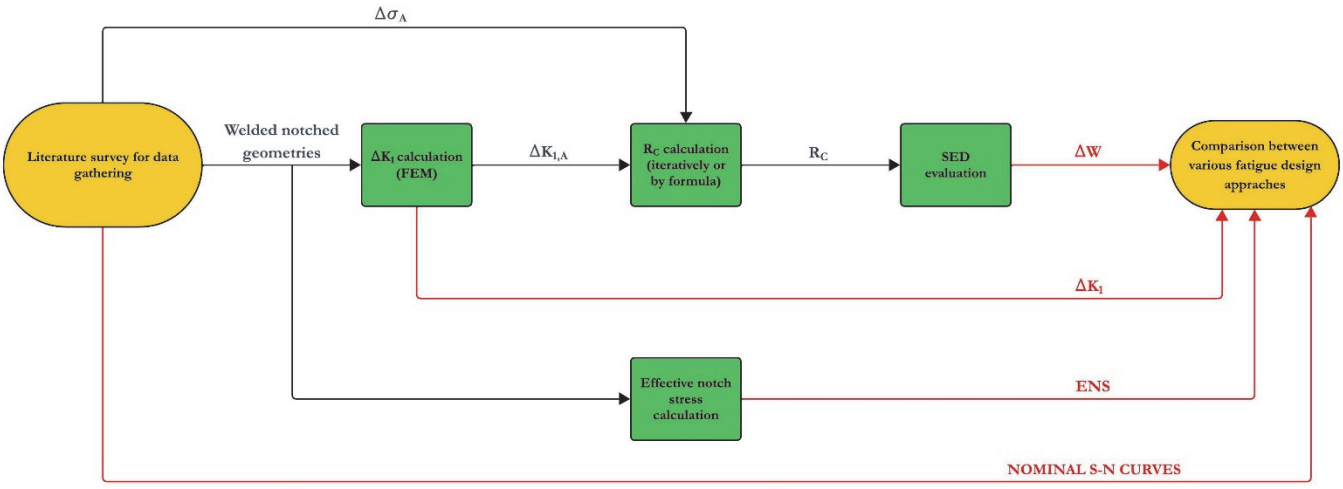

Figure 9: Flowchart of the present work.

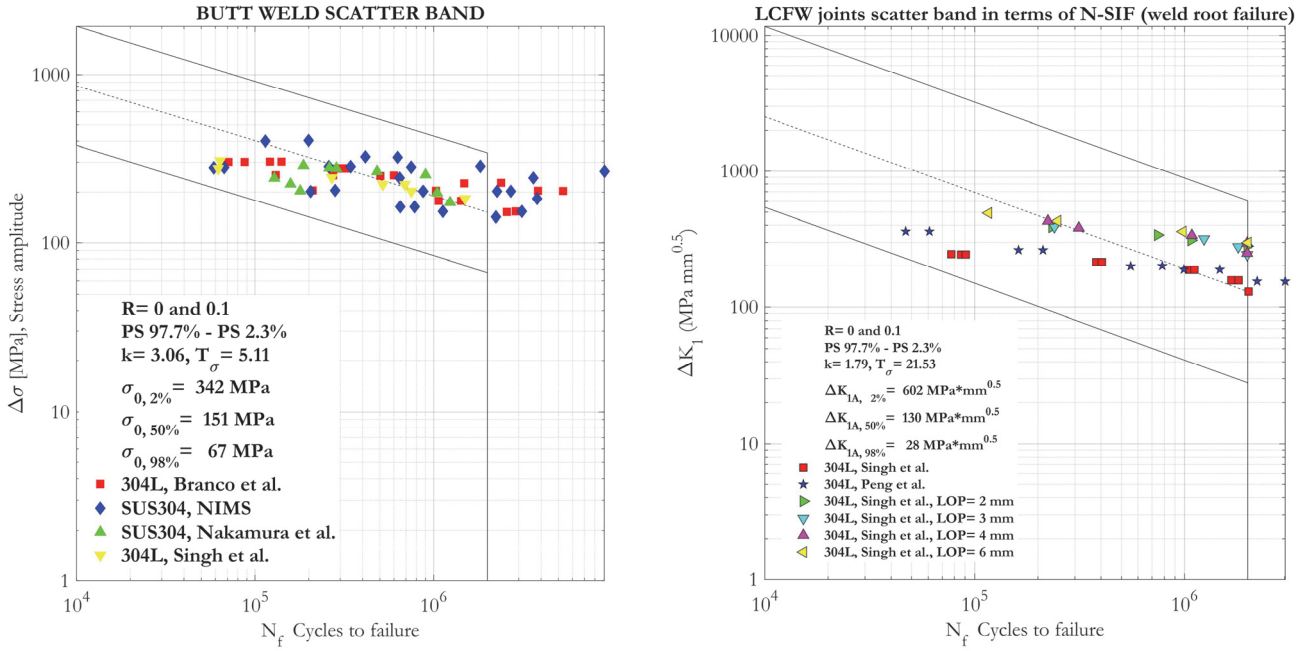

a) **b)**

Figure 10: Statistical analysis on fatigue data for: a) austenitic steel butt welded joints (nominal stress); b) austenitic steel cruciform LCFW joints (N-SIF).

RESULTS AND DISCUSSION

Fatigue limits estimation

Fig. 10a reports the results of the statistical analysis of fatigue data relating for austenitic steel butt ground welded joints, expressed in terms of nominal stress, based on a total of 63 data points. The fatigue limit associated with the mean design curve (P.S. 50%) $\Delta\sigma_{A,50\%}$, estimated at $2x10^6$ cycles, is equal to 151 MPa. Conversely, Fig. 10b shows the fatigue life, expressed in terms of N-SIF at the weld root, of the investigated austenitic steel load carrying cruciform welded joints. A total of 37 data points were included in the analysis. As explained previously, the fatigue limit $\Delta K_{1,A}$ is determined at $2x10^6$ cycles and is equal to 130 MPa $mm^{0.5}$.

SED critical radius evaluation

Once $\Delta\sigma_A$ and $\Delta K_{1,A}$ are determined, Eqn. 6 can be applied to calculate the critical radius R_C.
For a notch opening angle $2\alpha=0°$, e_1 is equal to 0.133 [15] and λ_1 is equal to 0.5 [8]. The application of this formula results in a critical radius value of 0.1954 mm. Moreover, for comparison purposes, an estimation of R_C was obtained by applying the iterative method on the geometry proposed by Singh et al. [23], considering all the SED values at $2x10^6$ while varying the control radius in the range 0.1 mm – 0.5 mm. The critical radius obtained from this approach is equal to 0.219 mm (Fig. 11), which differs by 10% from the one estimated with Eqn. 6. Nonetheless, R_C= 0.1954 mm is adopted for the following SED calculations, being it more conservative and aligned with the theoretical formulation.

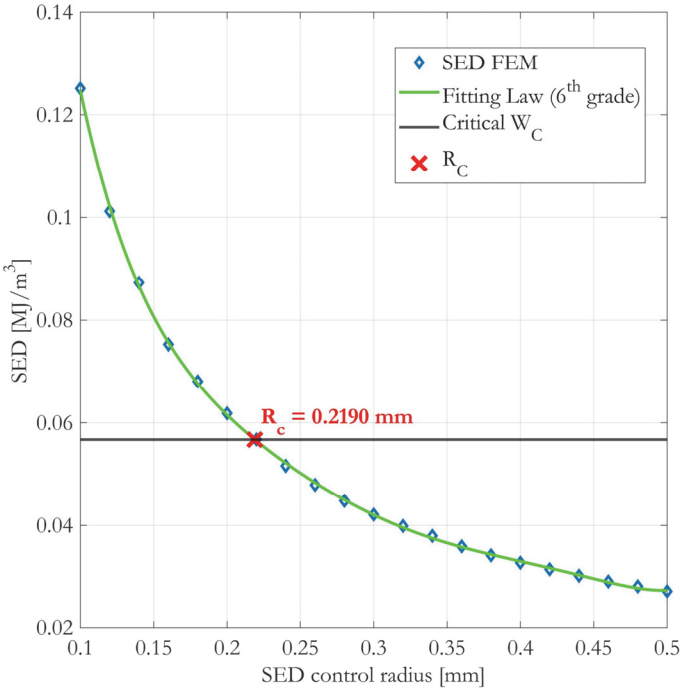

Figure 11: Calculation of SED critical radius with the "iterative" method.

ENS validation

Results of the ENS calculation and their comparison with the IIW FAT classes (negative inverse slope factor k=3) are displayed in Fig. 12a. Although most data points lie on or above the fatigue design curve (FAT 225) prescribed by the IIW, a pronounced scatter T_σ is observed, with several points exhibiting very high ENS values. This dispersion, shown in Fig. 12b, may stem from both material-specific effects, since austenitic stainless steels differ from the structural steels for which the method has been mainly calibrated, and the relatively strong geometrical modification introduced by the fictitious notch radius at the weld root, which may have led to an excessive reduction of the effective cross-section [7], despite joint geometries being compliant with the IIW thickness applicability limit of t,a≥5 mm. It is worth noting that the outlier points (triangles) are referred to the joint geometry proposed by Singh [25] (see Tab. 2), which is characterized by the smallest cross-section, and, more specifically, the most scattered points (yellow triangles) refer to the configuration in which the LOP defect length is equal to the plate thickness (LOP=a). The remaining points, for which the effect of the fictitious notch

radius is less impactful, fall within the band defined between the FAT 200 and FAT 300. Ultimately, a larger and more diverse dataset including failures initiating at the weld toe and joint geometries spanning different size scales is required to further assess the transferability of the ENS approach to austenitic stainless steels and to quantify its actual sensitivity to geometric parameters.

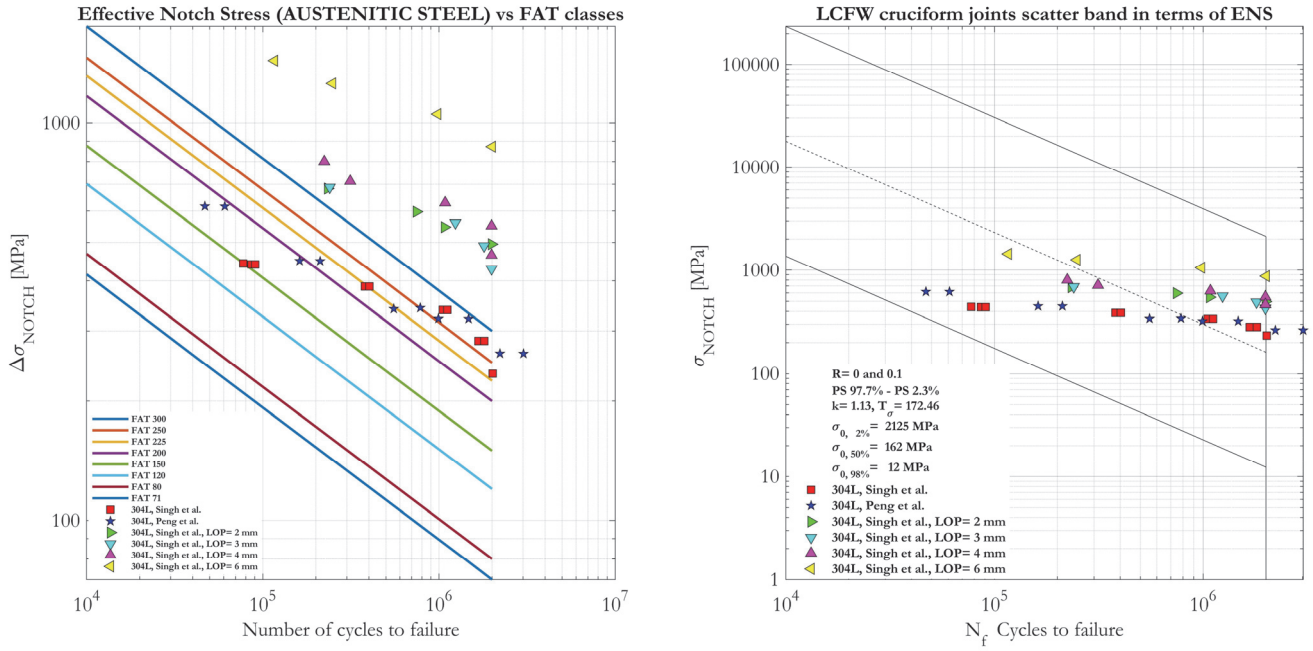

a) b)

Figure 12: Effective notch stress of austenitic steel LCFW cruciform joints: a)comparison with IIW FAT classes; b)statistical analysis

Effect of the fatigue parameter on data scatter: nominal stress, N-SIF and SED

Fig. 13 reports a comparison between the fatigue life of the analysed austenitic steel welded joints expressed in terms of nominal stress (Fig. 13a) and by N-SIF (Fig. 13b) and SED (Fig. 13c). In accordance with what is reported in the literature for other materials, a noticeable decrease in the data scatter is evidenced when moving from nominal stress (T_σ = 105) to local parameters-based representations. The SED scatter band index was expressed in terms of equivalent stress $T_{\sigma_{eq}} = \sqrt{T_W} = 19.51$.

SED-based fatigue life exhibits a slightly lower scatter index value than NSIF-based one (T_{NSIF}=21.53) and, in addition, enables the direct comparison of data coming from different types of joint, notch opening angles and load ratios.

Overall, N-SIF and SED approaches appear to provide a more unified treatment of the fatigue behaviour of austenitic steel welded structures, despite the limited and heterogeneous dataset considered.

A more solid validation could be achieved by enriching the current dataset with a sufficiently large and diverse number of data points.

Discussion

Fatigue is one of the most widespread damage mechanisms in structures and engineering components. The fatigue characterization of a material is a time and resource consuming process. Indeed, to obtain a Wöhler (S-N) curve, fatigue tests must be performed at different load levels, each of which should be repeated multiple times in order to obtain reliable results. In addition, experimental fatigue data expressed in terms of nominal stress are typically affected by scatter, arising from factors such as calibration uncertainties, imperfections in specimen geometry, testing machine alignment, electronic noise, as well as variations in chemical composition, impurity levels, and the size and distribution of microscopic defects[26]. This scatter becomes even more pronounced in components such as welded joints, where the damage mechanism is strongly influenced by the weld bead characteristics, such as geometry, mechanical properties of the welded material and the extent of the heat affected zone [28]. In this context, numerical methodologies can represent valuable tools in reducing time, cost and uncertainty in fatigue characterization. Among these, local approaches, such as N-SIF, SED and ENS, describe fatigue behaviour through parameters evaluated in the vicinity of the weld notch. These approaches have been successfully validated

for various materials but, to date, their applicability to austenitic stainless steel welded joints has not been thoroughly investigated.

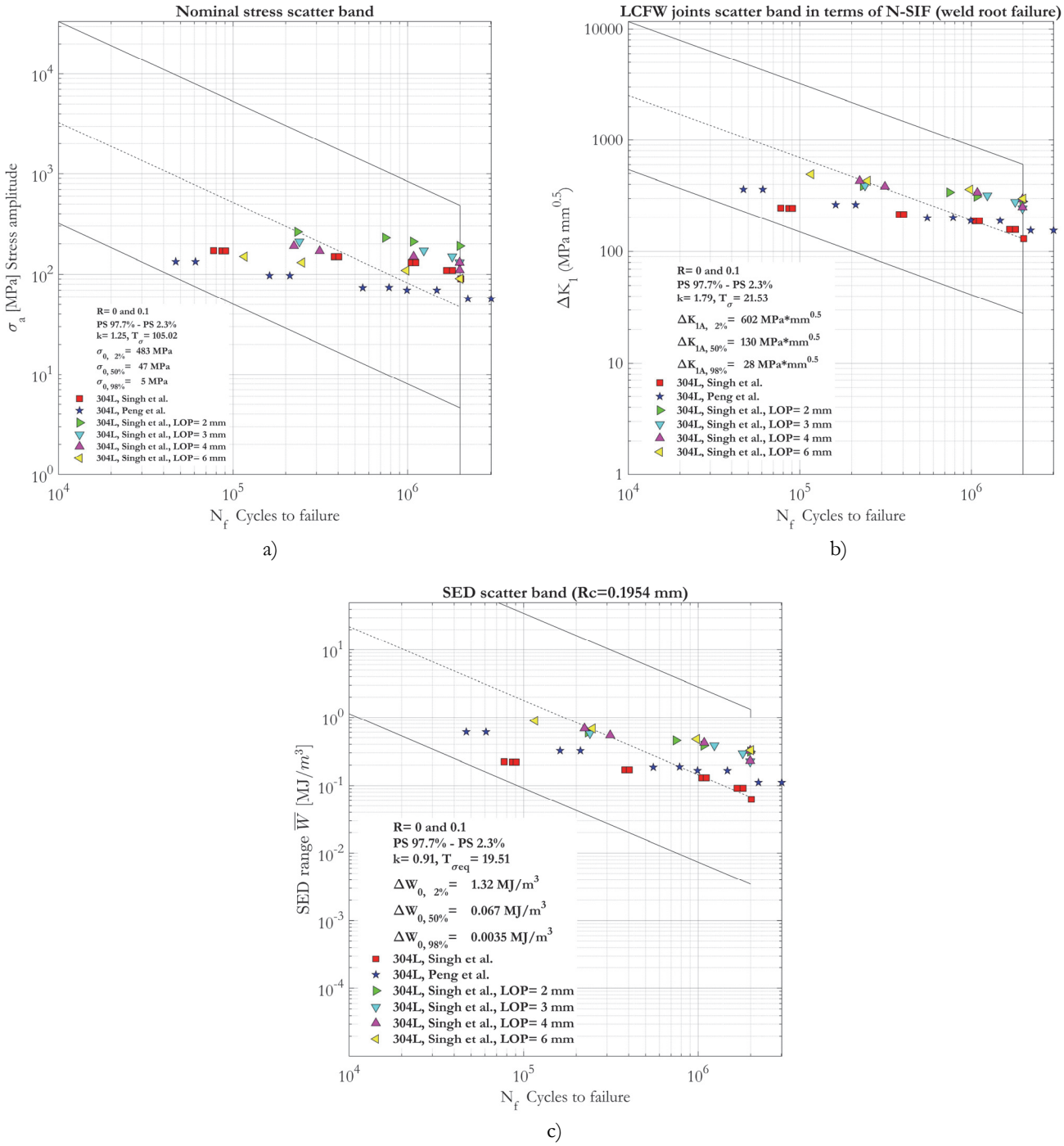

Figure 13: Fatigue life of austenitic steel welded joints expressed in terms of: a) nominal stress; b) N-SIF; c) SED

This work represents an initial step toward the applicability of N-SIF, SED and ENS to austenitic steel welded joints. In line with previous literature on other materials [29–33], the results obtained in the present study showed a significant reduction in fatigue data scatter when N-SIF and SED are applied, highlighting the capability of local parameters derived from fracture mechanics and energy-based formulations to provide a more unified treatment of different geometries and loading conditions. Conversely, the ENS approach exhibited a more pronounced dispersion in the analysed dataset, especially for thin joints characterised by smaller plate thickness and larger LOP length. This suggests that its applicability

to austenitic stainless steel welded joints may require further assessment, particularly when the relative size of the fictitious radius becomes non-negligible with respect to the joint thickness.
Finally, the main limitation of the present work lies in the size and heterogeneity of the available dataset, which is restricted to cruciform welded joints failing at the weld root. Although the trends observed are consistent with those reported in the literature for other materials, further experimental investigations including different joint typologies, failure locations and loading conditions are required to fully assess the robustness and transferability of the considered local approaches.

CONCLUSIONS

The present study is as a preliminary attempt to apply the numerical methodologies N-SIF, SED and ENS, already validated for other materials such as structural steel or aluminium, to the fatigue assessment of austenitic steel welded joints. Fatigue data on butt ground and cruciform austenitic steel welded joints acquired from the literature were implemented to calibrate the 2-D parametric finite element models. An initial set of simulations was performed to express the nominal stress-based fatigue data of cruciform welded joints in terms of N-SIF. After having determined both the fatigue limit of the plain welded material ($\Delta\sigma_A$ = 151 MPa) and the fatigue limit of the notched specimen expressed in terms of N-SIF (ΔK_{1A}=130 MPa*mm$^{0.5}$), the material characteristic length was calculated, resulting in R_C= 0.1945 mm and the proper SED control volume was applied to the finite element model. A second set of simulations was, then, carried out to obtain the SED-base representation of the fatigue data. Finally, by means of a second finite element model, the fatigue data were also re-elaborated in terms of ENS.
Statistical analysis of the various representations of fatigue life highlighted, in agreement with previous studies on other materials, an evident scatter reduction as the representation shifts from nominal stress-based to NSIF and SED-based. The ENS method, on the other hand, exhibited a pronounced dispersion of results for the joints, possibly due to material-specific effects and to the geometric regularisation introduced by the fictitious notch radius.
Overall, the adoption of local parameters seems to provide a more standardised procedure for the fatigue assessment of austenitic steel welded joint. More specifically, SED approach allows a straightforward comparison between data obtained from different joint geometry and load ratios. Nevertheless, the limited size and scope of the analysed dataset prevent any definitive conclusions from being drawn. Further developments of this work involve the implementation of a larger and more diversified experimental database (which accounts for different joint typologies, failure locations and size scales) in order to consolidate the applicability of the N-SIF and SED approaches and, where appropriate, to reconsider the applicability of the ENS method.

NOMENCLATURE

Latin

a	Vertical plate thickness
A	S-N curves intercept in the log-log domain
b	Weld bead length
B	Inverse slope of S-N curves in the log-log domain
C	Confidence level
c_w	Stress range correction factor
E	Young's modulus
e_1	Parameter depending on the notch opening angle
e_2	Parameter depending on the notch opening angle
ENS	Effective Notch Stress
FAT	Fatigue Strength Classes
FEA	Finite Element Analysis
GMAW	Gas Metal-Arc Welding
GTAW	Gas Tungsten-Arc Welding
IIW	International Institute of Welding
k	Negative inverse slope of S-N curves in the log-log domain
$k_{P.S,C}$	One-sided tolerance limit factor
K_1	Mode I Notch-Stress Intensity Factor

K_2	Mode II Notch-Stress Intensity Factor
L1	Horizontal plate length
L2	Vertical plate length
LCFW	Load carrying fillet weld
LOP	Lack of Penetration defect length
$\bar{N}$	Mean number of cycles
N-SIF	Notch-Stress Intensity Factor
P.S.	Survival probability
R	Load ratio
R_C	Strain energy density characteristic length
s_x	Standard deviation
SED	Strain energy density
T	Scatter band amplitude
t	Horizontal plate thickness
V	SED finite material volume

Greek

2α	Notch opening angle
$\Delta\sigma_A$	Fatigue limit of the base material
$\Delta\sigma_{A,50\%}$	Mean S-N curve fatigue limit
$\Delta\bar{W}$	Averaged cyclic strain energy density
ΔW_N	Cyclic SED value at the fatigue limit
ΔK_{1A}	Mode I N-SIF at the fatigue limit
ΔK_{2A}	Mode II N-SIF at the fatigue limit
ΔW_N	Cyclic SED of the base material at the fatigue limit
λ_1	Mode I Williams' eigenvalue
λ_2	Mode II Williams' eigenvalue
$\bar{\sigma}$	Mean stress
$\sigma_{P.S.,C}$	Stress probability limit
$\sigma_{\theta\theta}$	Normal stress component in a cylindrical coordinate system
$\tau_{r\theta}$	Shear stress component in a cylindrical coordinate system
ν	Poisson's ratio

REFERENCES

[1] Fricke, W. (2003). Fatigue analysis of welded joints: state of development, Mar. Struct., 16(3), pp. 185–200, DOI: https://doi.org/10.1016/S0951-8339(02)00075-8.

[2] Fan, J.L., Guo, X.L., Wu, C.W., Zhao, Y.G. (2011). Research on fatigue behavior evaluation and fatigue fracture mechanisms of cruciform welded joints, Mater. Sci. Eng. A, 528(29–30), pp. 8417–8427, DOI: https://doi.org/10.1016/j.msea.2011.08.037.

[3] Hobbacher, A.F. (2016). Recommendations for Fatigue Design of Welded Joints and Components, Cham, Springer International Publishing.

[4] British Standard Institution. (2015). Guide to fatigue design and assessment of steel products, DOI: https://doi.org/10.3403/30102063.

[5] (2005). EN 1993-1-9: Eurocode 3: Design of steel structures - Part 1-9: Fatigue.

[6] Lazzarin, P., Tovo, R. (1998). A notch intensity factor approach to the stress analysis of welds, Fatigue Fract. Eng. Mater. Struct., 21(9), pp. 1089–1103, DOI: https://doi.org/10.1046/j.1460-2695.1998.00097.x.

[7] Fricke, W. (2012). IIW Recommendations for the Fatigue Assessment of Welded Structures By Notch Stress Analysis: IIW-2006-09, IIW Recomm. Fatigue Assess. Welded Struct. By Notch Stress Anal. IIW-2006-09, pp. 1–41, DOI: https://doi.org/10.1533/9780857098566.

[8] Williams, M.L. (1952). Stress Singularities Resulting From Various Boundary Conditions in Angular Corners of Plates in Extension, J. Appl. Mech., 19(4), pp. 526–528, DOI: https://doi.org/10.1115/1.4010553.

[9] Gross, B., Mendelson, A. (1972). Plane elastostatic analysis of V-notched plates, Int. J. Fract. Mech., 8(3), pp. 267–276, DOI: https://doi.org/10.1007/BF00186126.
[10] Lazzarin, P., Zambardi, R. (2001). A finite-volume-energy based approach to predict the static and fatigue behavior of components with sharp V-shaped notches, Int. J. Fract., 112(3), pp. 275–298, DOI: https://doi.org/10.1023/A:1013595930617.
[11] Lazzarin, P., Berto, F., Zappalorto, M. (2010). Rapid calculations of notch stress intensity factors based on averaged strain energy density from coarse meshes: Theoretical bases and applications, Int. J. Fatigue, 32(10), pp. 1559–1567, DOI: https://doi.org/10.1016/j.ijfatigue.2010.02.017.
[12] Livieri, P., Lazzarin, P. (2005). Fatigue strength of steel and aluminium welded joints based on generalised stress intensity factors and local strain energy values, Int. J. Fract. 2005 1333, 133(3), pp. 247–276, DOI: https://doi.org/10.1007/s10704-005-4043-3.
[13] Meneghetti, G., Campagnolo, A., Berto, F., Tanaka, K. (2018). Notched Ti-6Al-4V titanium bars under multiaxial fatigue: Synthesis of crack initiation life based on the averaged strain energy density, Theor. Appl. Fract. Mech., 96, pp. 509–533, DOI: https://doi.org/10.1016/j.tafmec.2018.06.010.
[14] Berto, F. (2015). Local approaches for the fracture assessment of notched components: the research work developed by Professor Paolo Lazzarin, Fract. Struct. Integr., 9(34), pp. 11–26, DOI: https://doi.org/10.3221/IGF-ESIS.34.02.
[15] Livieri, P., Lazzarin, P. (2005). Fatigue strength of steel and aluminium welded joints based on generalised stress intensity factors and local strain energy values, Int. J. Fract., 133(3), pp. 247–276, DOI: https://doi.org/10.1007/s10704-005-4043-3.
[16] Crisafulli, D., Foti, P., Berto, F., Risitano, G., Santonocito, D. (2025). An innovative and sustainable methodology for fatigue characterization and design, Eng. Fract. Mech., 315, DOI: https://doi.org/10.1016/j.engfracmech.2025.110854.
[17] Lazzarin, P., Sonsino, C.M., Zambardi, R. (2004). A notch stress intensity approach to assess the multiaxial fatigue strength of welded tube-to-flange joints subjected to combined loadings, Fatigue Fract. Eng. Mater. Struct., 27(2), pp. 127–140, DOI: https://doi.org/10.1111/j.1460-2695.2004.00733.x.
[18] Lazzarin, P., Lassen, T., Livieri, P. (2003). A notch stress intensity approach applied to fatigue life predictions of welded joints with different local toe geometry, Fatigue Fract. Eng. Mater. Struct., 26(1), pp. 49–58, DOI: https://doi.org/10.1046/j.1460-2695.2003.00586.x.
[19] NIMS. NIMS.(n.d.). Data Sheets on Fatigue Crack Propagation Properties for Butt Welded Joints.
[20] Nakamura, Y., Chihiro, I., Mimura, H. (2009). Research on for Fatigue Strength of Austenitic Stainless Steel (Effects of Stress Ratio and Corrositive Environment), Kou Kouzou Rombunshuu (In Japanese).
[21] Branco C.M. , Maddox S.J., S.C.M. (1998). European Commission Science Research Development technical steel research Fatigue design of welded stainless steels.
[22] Singh, P.J., Guha, B., Achar, D.R.G. (2003). Fatigue life prediction for AISI 304L butt welded joints having different bead geometry using local stress approach, Sci. Technol. Weld. Join., 8(4), pp. 303–308, DOI: https://doi.org/10.1179/136217103225010934.
[23] Johan Singh, P., Guha, B., Achar, D.R.G. (2003). Fatigue life improvement of AISI 304L cruciform welded joints by cryogenic treatment, Eng. Fail. Anal., 10(1), pp. 1–12, DOI: https://doi.org/10.1016/S1350-6307(02)00033-X.
[24] Peng, Y., Dai, Z., Chen, J., Ju, X., Dong, J. (2021). Fatigue behaviour of load-carrying fillet-welded cruciform joints of austenitic stainless steel, J. Constr. Steel Res., 184, DOI: https://doi.org/10.1016/j.jcsr.2021.106798.
[25] Singh, P.J., Achar, D.R.G., Guha, B., Nordberg, H. (2002). Fatigue life prediction of gas tungsten arc welded AISI 304L cruciform joints with different LOP sizes, Int. J. Fatigue, 25(1), pp. 1–7, DOI: https://doi.org/10.1016/S0142-1123(02)00067-1.
[26] Dowling, N.E. (2013).Statistical Variation in Materials Properties. Mechanical Behavior of Materials: Engineering Methods for Deformation, Fracture, and Fatigue 4th ed., Pearson / Prentice Hall, pp. 900–907.
[27] Natrella, M.G. (1963). Experimental Statistics, Washington, DC, U.S. Government Printing Office.
[28] Taylor, D. (2002). Some new methods for predicting fatigue in welded joints, Int. J. Fatigue, 24(5), pp. 509–518, DOI: https://doi.org/10.1016/S0142-1123(01)00174-8.
[29] Berto, F., Campagnolo, A., Chebat, F., Cincera, M., Santini, M. (2016). Fatigue strength of steel rollers with failure occurring at the weld root based on the local strain energy values: modelling and fatigue assessment, Int. J. Fatigue, 82, pp. 643–657, DOI: https://doi.org/10.1016/j.ijfatigue.2015.09.023.
[30] Lazzarin, P., Livieri, P., Berto, F., Zappalorto, M. (2008). Local strain energy density and fatigue strength of welded joints under uniaxial and multiaxial loading, Eng. Fract. Mech., 75(7), pp. 1875–1889, DOI: https://doi.org/10.1016/j.engfracmech.2006.10.019.
[31] Foti, P., Berto, F. (2020). Fatigue assessment of high strength welded joints through the strain energy density method,

Fatigue Fract. Eng. Mater. Struct., 43(11), pp. 2694–2702,
DOI: https://doi.org/10.1111/FFE.13336;WGROUP:STRING:PUBLICATION.

[32] Berto, F., Campagnolo, A., Chebat, F., Cincera, M., Santini, M. (2016). Fatigue strength of steel rollers with failure occurring at the weld root based on the local strain energy values: modelling and fatigue assessment, Int. J. Fatigue, 82, pp. 643–657, DOI: https://doi.org/10.1016/J.IJFATIGUE.2015.09.023.

[33] Berto, F., Lazzarin, P. (2014). Fatigue strength of Al7075 notched plates based on the local SED averaged over a control volume, Sci. China Physics, Mech. Astron., 57(1), pp. 30–38, DOI: https://doi.org/10.1007/s11433-013-5275-2.